Ammoxidation of propene over antimony-vanadium-oxide catalysts

Roland Nilsson [a], Thomas Lindblad [b] and Arne Andersson [a,1]
[a] *Department of Chemical Engineering II and*
[b] *Department of Inorganic Chemistry 1, University of Lund, Chemical Center,*
PO Box 124, S-221 00 Lund, Sweden

Received 20 April 1994; accepted 20 September 1994

Antimony-vanadium-oxide catalysts were prepared with various Sb/V ratios and were used for propene ammoxidation. It was observed that antimony in excess of the amount required for forming $SbVO_4$ was required to have a catalyst that is selective to acrylonitrile formation. Characterisation of catalysts with FTIR revealed partial reduction of the oxidised phase $Sb_{0.92}V_{0.92}O_4$ upon use to form $Sb_{0.95}V_{1.05}O_4$. XPS data showed the surfaces of most selective catalysts to be further enriched with antimony in course of the catalytic reaction, thereby creating a surface structure that is selective. For acrylonitrile formation a yield of 55% was obtained at 90% of conversion. In propene oxidation, on the other hand, the yield for acrolein formation was limited to 20% due to consecutive combustion of the aldehyde.

Keywords: propene ammoxidation; propene oxidation; antimony-vanadium-oxides; XPS; FTIR

1. Introduction

For ammoxidation and oxidation of propene to acrylonitrile and acrolein, respectively, the bismuth molybdate and USb_3O_{10}/Sb_2O_4 catalyst systems are active and are used in the SOHIO process for the manufacture of the nitrile [1–3]. However, also the rutile systems SnO_2/Sb_2O_4 and $FeSbO_4/Sb_2O_4$ are active for allylic oxidation [4]. The pure rutiles SnO_2 and $FeSbO_4$, though active, are unselective in propene oxidation and ammoxidation, whereas Sb_2O_4 is selective but has low activity [5–8]. There is a general agreement that the rutile based catalysts have to be prepared with an excess of antimony oxide to obtain a catalyst that is both active and selective for allylic oxidation. The role of the excess antimony oxide has been a subject of many investigations and the hypotheses on the nature of the active sites on both rutiles generally fall in the four categories (i) a solid solution of Sb in the rutile [5,9], (ii) an oriented film or crystals of Sb_2O_4 grown on the surface

---

[1] To whom correspondence should be addressed.

of the rutile phase [6,10–12], (iii) surface modification [8,13] and Sb(V)=O surface sites [9,14], and (iv) phase interface effects [7,12].

A related catalyst system is $SbVO_4/Sb_2O_4$, which is a constituent in catalysts being active and selective for the ammoxidation of propane to acrylonitrile [15–18]. $SbVO_4$ is a cation deficient rutile with the composition $Sb_{0.92}V_{0.92}O_4$ when prepared in air [19]. It was reported that Sb_2O_4 in excess of the amount required for forming the rutile phase greatly improves the selectivity to acrylonitrile [16,18]. A similar observation for the oxidation of propene to acrolein was indicated in a note by Berry and Brett [20]. The $SbVO_4/Sb_2O_4$ system is also active for propene ammoxidation since propene was shown to be an intermediate in the reaction pathway from propane to acrylonitrile [18]. Considering previous works on this system mainly have concerned propane ammoxidation, the present investigation on propene ammoxidation and oxidation was undertaken. Catalysts, both freshly prepared and after use in the reactor, have been characterised with FTIR and XPS. To rationalise our understanding about the Sb-rutile systems for allylic oxidation, the present results are compared with those previously reported in the literature for the SnO_2/Sb_2O_4 and $FeSbO_4/Sb_2O_4$ systems.

2. Experimental

2.1. CATALYST PREPARATION

Catalysts with different Sb/V ratios were prepared by adding Sb_2O_3 to a warm solution of NH_4VO_3 in water. The mixture was heated under reflux for 16–18 h and the bulk of the water was then evaporated on a hot plate whilst stirring until a thick paste was formed. Residual water was removed by drying first at 110°C for 16 h and then at 350°C for 5 h. After sieving, the fraction of particles within the range 0.150–0.425 mm was calcined in a flow of air at 610°C for 3 h. From here on the catalysts are denoted SbxVy, where x/y is the Sb/V atomic ratio.

For comparative purposes oxidised $SbVO_4$, or more correct $Sb_{0.92}V_{0.92}O_4$ [19], was prepared form powders of V_2O_5 and Sb_2O_3 that were mixed and calcined in air at 800°C for 2 h. The reduced phase of the approximate composition $Sb_{0.95}V_{1.05}O_4$ [21,22] was prepared by heating the mixed powders in nitrogen free of oxygen also at 800°C for 2 h.

2.2. CATALYST CHARACTERISATION

A plug-flow reactor made of glass was used for the activity measurements. The catalyst sample was diluted with quartz grains to have isothermal conditions. Nitrogen, oxygen, ammonia, propene and water were dosed using mass flow controllers. The products were analysed on a gas chromatograph equipped with a sampling valve, an FID detector, a Porapak Q column and a methanation unit for the analysis of carbon oxides.

Transmission FTIR spectra of catalyst samples were recorded on a Nicolet 20 SXC instrument with a DTGS detector and a CsI beamsplitter. The resolution was 2 cm^{-1} and 1000 scans were averaged. Self-supporting discs were pressed, containing 3 mg of the sample diluted with 200 mg of KBr.

XPS measurements were performed on a Kratos XSAM 800 instrument using Mg Kα radiation (1253.6 eV). The samples were finely divided and then attached to the sample holder on a double-sided tape. Charging effects were overcome by mixing the samples with acetylene black (Carbon philblack 1-ISAF, supplied by Nordisk Philblack AB). The C 1s signal is at 284.3 eV and was used as reference. Two spectra with and without carbon black standard, respectively, were collected for each catalyst. The spectrum for the undiluted sample was used to calculate the Sb/V ratio, while the spectrum for the diluted sample was used to deduce the band positions unaffected by charging effects. Spectra for the Sb 3d, O 1s, V 2p, C 1s and Sb 4d regions were collected. For determination of the metal ratio the Sb $3d_{3/2}$ and V $2p_{3/2}$ bands were used since the Sb $3d_{5/2}$ band coincides with the O 1s band and the V $2p_{1/2}$ band is weak for samples with low content of vanadium. Therefore, the theoretical sensitivity factors were recalculated and set as Sb 3d = 3.20 and V 2p = 1.30.

3. Results

3.1. AMMOXIDATION OF PROPENE

The dependences on catalyst composition of the total reaction rate and the rates and selectivities for the formations of acrylonitrile, acrolein, acetonitrile and carbon oxides are shown in fig. 1. Hydrogen cyanide and small amounts of methane, ethene, and propane were also produced. The total reaction rate and the rates for formation of carbon oxides, acrylonitrile and acetonitrile show maxima for 33.3 at% Sb (Sb1V2). In contrast to this, the rate for formation of acrolein is the highest for compositions rich in antimony. Considering the selectivities, it is observed that those to acrylonitrile and acrolein have maxima while that for carbon oxide formation has a slight minimum for compositions rich in antimony. The selectivity to acetonitrile decreases with increasing antimony content. Comparison shows no significant difference in rates and selectivities for Sb1V1 and $Sb_{0.92}V_{0.92}O_4$.

Fig. 2 shows the yields and the selectivities as a function of the conversion of propene for the Sb2V1 catalyst. The selectivity to acrylonitrile passes through a maximum of about 65% at conversions between 50 and 70%. For acrolein formation the selectivity decreases with increase in conversion. The selectivity to acetonitrile is almost independent of the conversion level and so is the selectivity to carbon oxi-

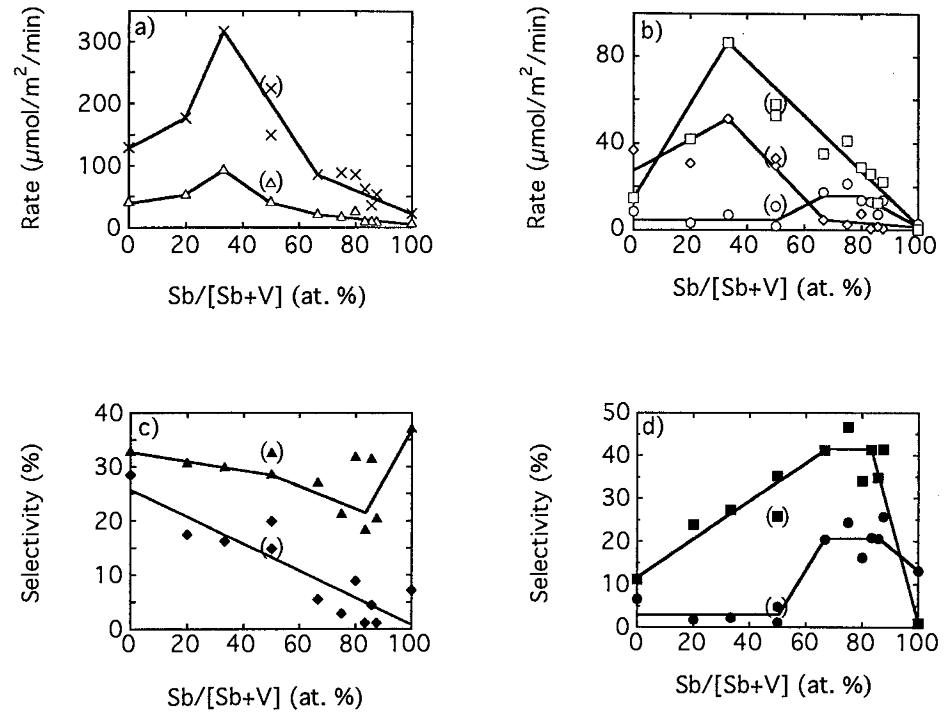

Fig. 1. Variation of rates and selectivities in propene ammoxidation with the antimony content. (a) Rates for propene conversion (×), and for the formation of carbon oxides (△). (b) Rates for formation of acetonitrile (◇), acrolein (○), and acrylonitrile (□). (c) Selectivities for formation of acetonitrile (◆), and carbon oxides (▲). (d) Selectivities for formation of acrolein (●), and acrylonitrile (■). Data within brackets are for $Sb_{0.92}V_{0.92}O_4$. Experimental conditions: reaction temperature 480°C, mole ratio propene/oxygen/ammonia/water vapour/nitrogen = 1/4/2/1/6, and propene conversion 4–8%.

des (~ 25%) up to 70% conversion. The yields for formation of acrylonitrile and carbon oxides increase with increase in conversion and are about 55 and 25%, respectively, at 90% conversion, while the yields for formation of acetonitrile and acrolein are low. Analysis showed that ammonia was still breaking through at high conversions of propene. This is in agreement with the finding that the yield for acrylonitrile formation increases almost linearly with increase in propene conversion.

3.2. OXIDATION OF PROPENE

The catalyst Sb2V1 was also tested for the oxidation of propene. Acrolein and carbon oxides are the main products and the yields and selectivities are shown in fig. 3 as a function of the propene conversion. The selectivity for formation of acrolein decreases with increasing conversion, whilst the selectivity towards carbon oxides increases. The yield for carbon oxide formation increases with the conversion and that for acrolein passes through a maximum of about 20% at conversions around 60%.

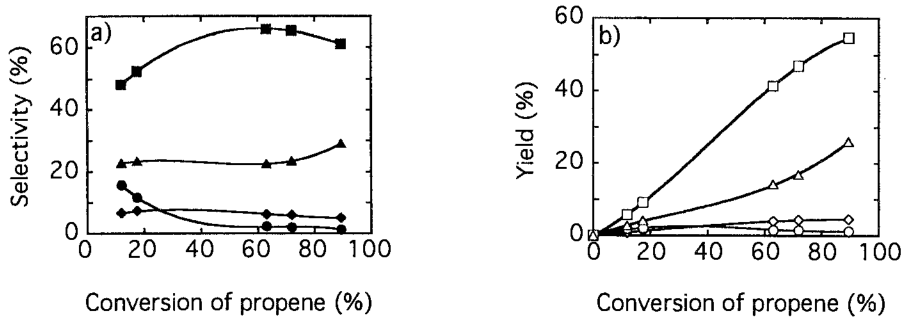

Fig. 2. Variation of selectivities and yields with propene conversion in the ammoxidation over Sb2V1. (a) Selectivities for formation of acetonitrile (◆), acrolein (●), acrylonitrile (■), and carbon oxides (▲). (b) Yields of acetonitrile (◇), acrolein (○), acrylonitrile (□), and carbon oxides (△). Experimental conditions: reaction temperature 480°C, mole ratio propene/oxygen/ammonia/water vapour/nitrogen = 1/4/2/1/6, total flow 70 ml/min (STP), and weight of catalyst 0.1–2.1 g.

3.3. FTIR CHARACTERISATION

In fig. 4 the infrared spectra are shown for the oxidised form ($Sb_{0.92}V_{0.92}O_4$) and the reduced form ($Sb_{0.95}V_{1.05}O_4$) of $SbVO_4$ together with the spectrum of α-Sb_2O_4. Spectra for $Sb_{0.92}V_{0.92}O_4$ are shown both before and after use in propene ammoxidation for 7 h. In the spectral region below 800 cm^{-1} the oxidised $SbVO_4$ (spectrum 1) gives bands at 362, 554 and 671 cm^{-1} together with a shoulder at 726 cm^{-1}, which are all typical for the rutile structure [23,24]. The reduced form of $SbVO_4$ (spectrum 3) has the same rutile bands, however, the spectrum reveals as well contamination with some α-Sb_2O_4 (cf. spectrum 4). In the region above 800 cm^{-1}, the oxidised form of $SbVO_4$ gives two typical bands at 880 and 1016 cm^{-1}, which are due to the 2-coordinated oxygen species that are present as a result of the cation deficient rutile structure [19]. The band at 1016 cm^{-1} has been assigned to a vanadyl group (V=O - - - Sb) and the band at 880 cm^{-1} was tenta-

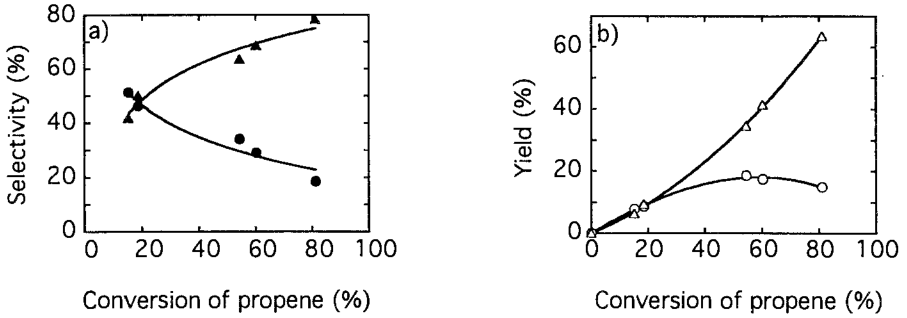

Fig. 3. Variation of selectivities and yields with propene conversion in the oxidation over Sb2V1. (a) Selectivities for formation of acrolein (●), and carbon oxides (▲). (b) Yields of acrolein (○), and carbon oxides (△). Experimental conditions: reaction temperature 480°C, mole ratio propene/oxygen/water vapour/nitrogen = 1/4/1/8, total flow 70 ml/min (STP), and weight of catalyst 0.1–2.1 g.

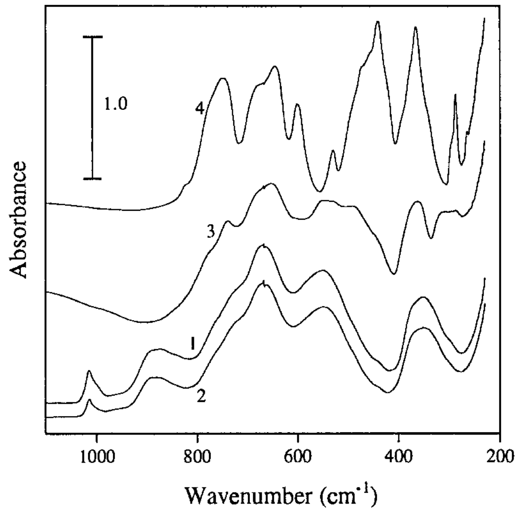

Fig. 4. FTIR spectra of $Sb_{0.92}V_{0.92}O_4$ before (1) and after (2) use in propene ammoxidation, $Sb_{0.95}V_{1.05}O_4$ (3), and α-Sb_2O_4 (4).

tively suggested to be from an (Sb–O–Sb) vibration mode [25]. The latter assignment was based on valence considerations, but a (V–O–V) vibration mode cannot be excluded to explain the 880 cm^{-1} band. The spectra of the two fresh preparations of $SbVO_4$ agree with the findings reported by other investigators [21,22], namely, that synthesis in air gives a pure oxidised phase, while preparation without gaseous oxygen gives the reduced phase contaminated with antimony oxide. Spectrum 2, which was recorded for $Sb_{0.92}V_{0.92}O_4$ after use in ammoxidation, shows the bands above 800 cm^{-1} to be somewhat less intense compared with those in spectrum 1 for the fresh sample, indicating partial reduction.

Some representative infrared spectra of catalysts are shown in fig. 5 both before and after use in propene ammoxidation for 7 h. The spectra for the fresh Sb1V2 and Sb1V1 samples show the features from oxidised $SbVO_4$ (cf. spectrum 1 in fig. 4) together with features from V_2O_5. The latter phase contributes to the absorbance at 1016 cm^{-1} and is responsible for the shift of the 880 cm^{-1} band to 840 cm^{-1} and for the appearance of bands at about 600, 480 (shoulder) and 298 cm^{-1} [26]. The XRD patterns of the samples confirmed this result and showed for Sb1V2 the presence of V_2O_5 and oxidised $SbVO_4$. For Sb1V1 the XRD reflections from oxidised $SbVO_4$ were dominant, but those from unreacted V_2O_5 and α-Sb_2O_4 were also clearly visible. After use in the ammoxidation the infrared bands from V_2O_5 have disappeared in both cases and comparison with the spectra in fig. 4 reveals that reduction of the $SbVO_4$ phase has occurred. In case of Sb1V1 (spectrum 4) the reduction is incomplete, because weak bands at 1016 and 880 cm^{-1} from oxidised $SbVO_4$ are still present. The reduction of Sb1V2 (spectrum 2) seems more severe.

The spectra for Sb3V1 and Sb6V1 are typical for samples with excess α-Sb_2O_4.

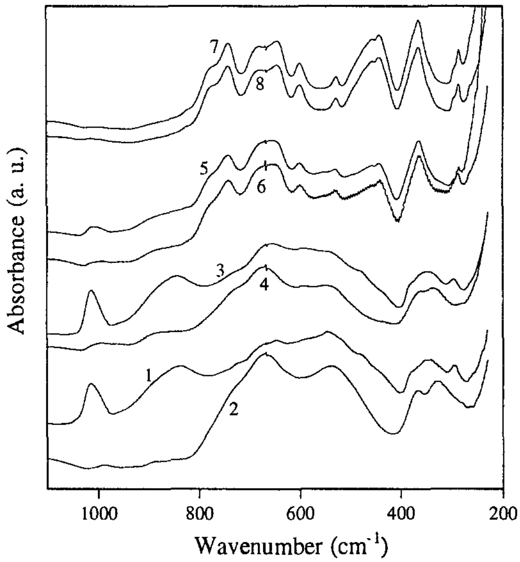

Fig. 5. FTIR spectra of representative catalyst samples before and after use in propene ammoxidation. Sb1V2, fresh (1) and used (2); Sb1V1, fresh (3) and used (4); Sb3V1, fresh (5) and used (6); and Sb6V1, fresh (7) and used (8).

Bands from both α-Sb_2O_4 and oxidised $SbVO_4$ are clearly apparent in the spectra of the fresh samples, although the bands from the latter phase are weak in the spectrum for Sb6V1 due to the large excess of α-Sb_2O_4. After catalytic tests the bands from α-Sb_2O_4 remain unchanged, but the typical bands for oxidised $SbVO_4$ at 1016 and 880 cm^{-1} have decreased in intensity due to reduction.

3.4. XPS CHARACTERISATION

XPS data measured for the fresh samples and after their use in propene ammoxidation for 7 h are given in table 1. The Sb $3d_{3/2}$ binding energy value is almost the same (540.1 eV) for fresh samples with the nominal compositions $Sb/V \leqslant 1$, and the value slightly decreases with further increase in antimony content. Moreover, for the samples with high vanadium contents the Sb $3d_{3/2}$ binding energy decreases upon use, while rather the reverse can be noticed for the samples that are rich in antimony.

Considering the V $2p_{3/2}$ signal for fresh catalysts, the binding energy is the highest for Sb1V4 and Sb1V2 and for the other samples, it is about 0.3 eV less. Upon use in ammoxidation, the V $2p_{3/2}$ signal broadens (cf. FWHM) and the peak maximum shifts towards binding energy values. For the samples with large excess of antimony the full width at half maximum (FWHM) could not be measured for V $2p_{3/2}$ due to the low intensity of the signal.

The Sb/V surface ratios measured by XPS show for the samples with $Sb/V \leqslant 1$ a decrease to occur upon use, while a corresponding increase is observed for the samples with excess antimony oxide.

Table 1
Core line binding energies, half widths[a] and Sb/V ratios determined by XPS for catalyst samples before and after use in propene ammoxidation

Sample	Sb/V atomic ratio			Sb $3d_{3/2}$[b] (eV)		V $2p_{3/2}$[c] (eV)	
	nominal	XPS, fresh	XPS, used	fresh	used	fresh	used
Sb1V4	1 : 4	1 : 1.4	1 : 2.0	540.1 (1.8)	539.8 (1.7)	517.0 (1.8)	516.2 (2.8)
Sb1V2	1 : 2	1 : 1.6	1 : 1.7	540.1 (1.6)	539.9 (1.7)	516.9 (2.0)	516.3 (2.7)
$SbVO_4$[d]	1 : 1	1.1 : 1	0.9 : 1	540.2 (1.8)	540.1 (1.7)	516.8 (2.2)	516.5 (2.5)
Sb1V1	1 : 1	1.1 : 1	0.9 : 1	540.1 (1.7)	540.1 (1.7)	516.7 (2.1)	516.5 (2.6)
Sb2V1	2 : 1	2.0 : 1	3.3 : 1	540.0 (1.8)	540.1 (2.2)	516.7 (2.2)	516.5 (2.4)
Sb3V1	3 : 1	2.6 : 1	4.8 : 1	539.9(2.0)	540.0 (2.1)	516.6 (2.2)	516.4 (2.4)
Sb4V1	4 : 1	3.8 : 1	4.8 : 1	539.8(2.1)	539.9 (2.2)	516.8 (2.3)	516.3 (2.7)
Sb5V1	5 : 1	12.6 : 1	33.3 : 1	539.8 (2.1)	539.9 (2.1)	516.6	516.3
Sb6V1	6 : 1	5.3 : 1	16.7 : 1	539.7 (1.9)	539.8 (2.1)	516.7	516.2
Sb7V1	7 : 1	9.7 : 1	50.0 : 1	539.8 (2.0)	539.9 (2.1)	516.6	516.3

[a] Given within brackets.

[b] The Sb $3d_{3/2}$ binding energies and half widths measured for α-Sb_2O_4, Sb_2O_5 (Aldrich) and $Sb_{0.95}V_{1.05}O_4$ were 539.9 (2.0), 540.3 (2.1) and 540.1 (2.2) eV, respectively.

[c] The V $2p_{3/2}$ binding energies measured for V_2O_5 and $Sb_{0.95}V_{1.05}O_4$ were 517.1 (1.4) and 516.0 (2.5) eV, respectively.

[d] Pure $Sb_{0.92}V_{0.92}O_4$.

4. Discussion

Considering the infrared spectra in fig. 5 it is obvious that oxidised $SbVO_4$, $Sb_{0.92}V_{0.92}O_4$, is a constituent in the freshly prepared catalysts. Moreover, V_2O_5 and α-Sb_2O_4 are present when $Sb/V<1$ and $Sb/V>1$, respectively. For Sb1V1, which was calcined at 610°C likewise the other catalyst preparations, the infrared spectrum reveals the presence of some unreacted V_2O_5 and the XRD pattern showed the presence of some α-Sb_2O_4 as well. Oxidised $SbVO_4$ prepared at 800°C is a single phase rutile. Thus, the results show that for complete reaction of vanadia to form $SbVO_4$ it is necessary to have either a high calcination temperature or excess of antimony oxide. The Sb $3d_{3/2}$ binding energy values in table 1 show predominance for Sb^{5+} surface states in fresh samples with $Sb/V \leqslant 1$, where the antimony mainly is in form of $Sb_{0.92}V_{0.92}O_4$. Mössbauer data [21] have shown the antimony in both $Sb_{0.92}V_{0.92}O_4$ and $Sb_{0.95}V_{1.05}O_4$ to be in the pentavalent state in the bulk. Consequently, the valences and the compositions for the oxidised and the reduced $SbVO_4$ can be expressed as $Sb(V)_{0.92}V(III)_{0.28}V(IV)_{0.64}O_4$ and $Sb(V)_{0.95}V(III)_{0.95}V(IV)_{0.10}O_4$, respectively. According to table 1 the V $2p_{3/2}$ binding energy values are about 516.7 eV with half widths of about 2.2 eV for the fresh samples with the vanadium largely in form of $Sb_{0.92}V_{0.92}O_4$. These values, when compared with those for pure V_2O_5, clearly indicate a contribution to the V $2p_{3/2}$ signal from V^{5+} surface states besides V^{4+} (and V^{3+}) sub-surface states.

The activity dependences in fig. 1 show two synergy effects. One is evident as activity maxima in the vanadia/$SbVO_4$ region (0–50 at% Sb). Both the total rate and the rates for the formations of acrylonitrile, acetonitrile and carbon oxides are the highest for Sb1V2 (33.3 at% Sb), inferring that the effect is related to the initial activation of propene, i.e., the adsorption or the abstraction of hydrogen. Whereas a corresponding effect was observed for the formation of propene from propane [25], the synergy effect probably is related to the hydrogen abstraction. According to the XPS data in table 1, the Sb/V surface ratio decreases upon use in ammoxidation of samples belonging to this composition region. The corresponding infrared spectra of used samples in fig. 5 show bands neither from V_2O_5 nor from any other crystalline vanadia phase. The results can be explained by the formation of amorphous vanadia, which to some extent has spread over the surface of $SbVO_4$ under influence of the catalytic process. Thus, the rate maxima can be due to either the amorphous phase itself or its interface with the $SbVO_4$ phase. Considering the changes of the Sb $3d_{3/2}$ and V $2p_{3/2}$ binding energies shown in table 1, it is obvious that both elements are reduced upon use in ammoxidation of the vanadia-rich samples, giving preference for the latter explanation involving phase cooperation. This interpretation also is in line with the fact that the XPS data and the infrared spectra after use of Sb1V2 and Sb1V1 show greater reduction of the former sample. The original V_2O_5 content of the latter sample was less and was due to the incomplete reaction with antimony oxide during the preparation.

A second synergy effect is apparent in fig. 1 as maxima for the selectivities to acrylonitrile and acrolein in the α-Sb_2O_4/$SbVO_4$ region (50–100 at% Sb). The comparatively lower selectivities to nitrile and aldehyde over Sb1V1 compared with the samples with α-Sb_2O_4 in excess are primarily not due to the fact that the freshly prepared Sb1V1 contained some unreacted V_2O_5, because the activity data in fig. 1 for low conversion levels show similar values for both Sb1V1 and the sample that was charged as pure $Sb_{0.92}V_{0.92}O_4$. However, with longer residence times it is known that the vanadia overlayer causes loss of selectivity due to the fact that it catalyses the conversion of NH_3 to N_2 [17,27]. The XPS data in table 1 show for the samples with excess α-Sb_2O_4 that the Sb/V surface ratio increases with use of the samples in ammoxidation. This observation indicates spreading of antimony oxide species from α-Sb_2O_4, having both Sb^{3+} and Sb^{5+} states, to the surface of $SbVO_4$, with preference for Sb^{5+} states, and interaction is confirmed by the trend toward increase of the Sb $3d_{3/2}$ binding energy after use. Simultaneous reduction of the oxidised phase $Sb(V)_{0.92}V(III)_{0.28}V(IV)_{0.64}O_4$ to form partly the reduced phase $Sb(V)_{0.95}V(III)_{0.95}V(IV)_{0.10}O_4$ is shown by the infrared spectra in fig. 5, where a decrease in intensity of the bands at 1016 and 880 cm^{-1} is evident after use of the samples. Additional support for reduction is the observed broadening and decrease in binding energy of the V $2p_{3/2}$ peak (table 1), indicating increased contribution to the signal from V^{3+} states. The V $2p_{3/2}$ binding energy for the used samples decreases when the nominal Sb/V ratio increases from 1 : 1 to 4 : 1 and is almost constant (516.3 eV) at higher ratios. The trend can be due to the coverage and interaction with the spread antimony oxide species of surface V^{5+} species, converting the latter to V^{4+} (V^{3+}) sub-surface species. Whereas the pure $SbVO_4$, Sb1V1 and α-Sb_2O_4 are not the most selective catalysts, it seems that the high selectivity for catalysts with both α-Sb_2O_4 and $SbVO_4$ partly is a consequence of the poisoning of V^{5+} sites with supra-surface antimony oxide species, resulting in less formation of degradation products (cf. fig. 1c). The decrease in selectivity to degradation with increase in antimony content matches the relative increase of the Sb/V ratio as determined by XPS for used samples, which changes from 1.65 (3.3/2.0) for Sb2V1 to 5.15 (50.0/9.7) for Sb7V1. An improved selectivity for $SbVO_4$ with excess α-Sb_2O_4 has as well been reported for the oxidation of propene [20] and for the ammoxidation of propane [16,18,25]. For the latter reaction spreading of antimony oxide was observed [18,25] and the synergy effect is consistent with the present results, considering that propene was found to be an intermediate from propane to acrylonitrile.

Extrapolation to zero propene conversion of the dependences depicted in fig. 2a shows the initial selectivity to be approximately 35% to both acrylonitrile and acrolein, while it is 20 and 5% for the carbon oxide and acetonitrile formation, respectively. It is thus obvious that all four products are to some extent initial products formed in parallel routes. The initial increase with conversion of the selectivity to acrylonitrile goes with a corresponding decrease of the selectivity to acrolein, showing that some nitrile is formed by conversion of the aldehyde with ammonia. Although the nitrile is a stable product, some of it is combusted as is evident considering that the decrease in the selectivity to nitrile at high conversion is matched by the increase in the selectivity to carbon oxides. Acetonitrile solely is a primary product and there is no indication of its formation from any other product.

For propene oxidation the variations in fig. 3 show that acrolein is the main primary product. Acrolein compared with acrylonitrile is less stable and reacts consecutively to form carbon oxides. An initial selectivity to acrolein of about 70% is estimated by extrapolating the selectivity variation in fig. 3a to zero propene conversion. This value is approximately equal to the sum of the initial selectivities to nitrile and aldehyde that was obtained from the ammoxidation data in fig. 2a, inferring that the same surface structure is active for both aldehyde and nitrile depending on whether it has an oxygen or an isoelectronic, dehydrogenated ammonia species. Such mechanistic features concur with those concluded for propene conversion over molybdate and Fe-Sb-oxide catalysts [28].

There are some difficulties comparing the performance of the $SbVO_4/Sb_2O_4$ system in propene oxidation and ammoxidation with the data reported for the SnO_2/Sb_2O_4 and $FeSbO_4/Sb_2O_4$ systems, since data are given for different reaction conditions. For propene oxidation over SnO_2/Sb_2O_4 [10,11] and $FeSbO_4/Sb_2O_4$ [7,8] selectivities as high as 70–80% were reported for acrolein formation at low conversion, while for propene ammoxidation over the former system an initial selectivity of 80% to acrylonitrile was observed [5]. The present data in fig. 3 for an Sb-V-oxide catalyst show similar values for acrolein formation when extrapolated to initial conditions. In propene ammoxidation over the $SbVO_4/Sb_2O_4$ system (cf. fig. 2) it seems that the consecutive transformation of acrolein to acrylonitrile plays a greater role than it does over the SnO_2/Sb_2O_4 system, where acrolein possibly is not an intermediate. Considering the present finding of antimony enrichment at the $SbVO_4$ surface as a prerequisite for having a selective catalyst, this is partly consistent with interpretations given for the other rutile systems that an oriented film or crystals of α-Sb_2O_4 form a site that is active for allylic oxidation. However, a difference is that the present results show that the supra-surface antimony sites on $SbVO_4$ predominantly are Sb^{5+} sites. For the SnO_2/Sb_2O_4 system it was proposed that the oriented film itself constitutes the active site [6,10,11], while for the $FeSbO_4/Sb_2O_4$ system Grasselli and coworkers [12] rather considered the possibility that the active site is at the interface region between α-Sb_2O_4 crystals and the rutile phase. On $SbVO_4$ the spread antimony oxide lowers the activity and increases the selectivity. Our observations suggest the role of the supra-surface antimony species to be of promoting character, leading to reconstruction of the $SbVO_4$ surface and blocking of V^{5+} sites active for degradation. This hypothesis has similarities as well with those considering modification with antimony of the SnO_2 [13,14] and $FeSbO_4$ [8,9,14] surfaces as explanation for the role of excess antimony oxide in allylic oxidation over rutiles.

Acknowledgement

Financial support from the Swedish Research Council for Engineering Sciences (TFR) and the National Board for Industrial and Technical Development (NUTEK) is gratefully acknowledged.

References

[1] R.K. Grasselli and J.D. Burrington, in: *Advances in Catalysis*, Vol. 30, eds. D.D. Eley, H. Pines and P.B. Weisz (Academic Press, New York, 1981) pp. 133–163.
[2] R.K. Grasselli and J.L. Callahan, J. Catal. 14 (1969) 93.
[3] R.K. Grasselli, G. Centi and F. Trifirò, Appl. Catal. 57 (1990) 149.
[4] G. Centi and F. Trifirò, Catal. Rev.-Sci. Eng. 28 (1986) 165.
[5] M. Crozat and J.-E. Germain, Bull. Soc. Chim. France (1973) 1125.
[6] J.C. Volta, P. Bussiere, G. Coudurier, J.M. Herrmann and J.C. Vedrine, Appl. Catal. 16 (1985) 315.
[7] V. Fattore, Z.A. Fuhrman, G. Manara and B. Notari, J. Catal. 37 (1975) 223.
[8] I. Aso, S. Furukawa, N. Yamazoe and T. Seiyama, J. Catal. 64 (1980) 29.
[9] M. Carbucicchio, G. Centi and F. Trifirò, J. Catal. 91 (1985) 85.
[10] Y. Boudeville, F. Figueras, M. Forissier, J.-L. Portefaix and J.C. Vedrine, J. Catal. 58 (1979) 52.
[11] F. Figueras, M. Forissier, J.P. Lacharme and J.L. Portefaix, Appl. Catal. 19 (1985) 21.
[12] R.G. Teller, J.F. Brazdil and R.K. Grasselli, J. Chem. Soc. Faraday Trans. I 81 (1985) 1693.
[13] H.J. Herniman, D.R. Pyke and R. Reid, J. Catal. 58 (1979) 68.

[14] F. Sala and F. Trifirò, J. Catal. 41 (1976) 1.
[15] US Patents 4,746,641 (1988); 4,788,317 (1988); 4,879,264 (1989); assigned to the Standard Oil Company, OH, USA.
[16] G. Centi, R.K. Grasselli, E. Patane and F. Trifirò, in: *New Developments in Selective Oxidation,* Studies in Surface Science and Catalysis, Vol. 55, eds. G. Centi and F. Trifirò (Elsevier, Amsterdam, 1990) pp. 515–526.
[17] A. Andersson, S.L.T. Andersson, G. Centi, R.K. Grasselli, M. Sanati and F. Trifirò, in: *Proc. 10th Int. Congr. on Catalysis,* Part A, eds. L. Guczi, F. Solymosi and P. Tétényi (Akadémiai Kiadó, Budapest, 1993) pp. 691–705.
[18] R. Nilsson, T. Lindblad, A. Andersson, C. Song and S. Hansen, in: *New Developments in Selective Oxidation II,* Studies in Surface Science and Catalysis, Vol. 82, eds. C. Corberán and S. Vic Bellón (Elsevier, Amsterdam, 1994) pp. 293–303.
[19] S. Hansen, K. Ståhl, R. Nilsson and A. Andersson, J. Solid State Chem. 102 (1993) 340.
[20] F.J. Berry and M.E. Brett, J. Catal. 88 (1984) 232.
[21] T. Birchall and A.W. Sleight, Inorg. Chem. 15 (1976) 868.
[22] F.J. Berry, M.E. Brett and W.R. Patterson, J. Chem. Soc. Dalton Trans. (1983) 9.
[23] C. Rocchiccioli-Deltcheff, T. Dupuis, R. Franck, M. Harmelin and C. Wadier, Compt. Rend. Acad. Sci. Paris B 270 (1970) 541.
[24] E. Husson, Y. Repelin, H. Brusset and A. Cerez, Spectrochim. Acta A 35 (1979) 1177.
[25] R. Nilsson, T. Lindblad and A. Andersson, J. Catal. 148 (1994) 501.
[26] L. Abello, E. Husson, Y. Repelin and G. Lucazeau, Spectrochim. Acta A 39 (1983) 641.
[27] A. Andersson, S.L.T. Andersson, G. Centi, R.K. Grasselli, M. Sanati and F. Trifirò, Appl. Catal. A 113 (1994) 43.
[28] J.D. Burrington, C.T. Kartisek and R.K. Grasselli, J. Catal. 87 (1984) 363.